Pharm Res (2012) 29:669–682
DOI 10.1007/s11095-011-0589-0

RESEARCH PAPER

Comparison of Polymeric siRNA Nanocarriers in a Murine LPS-Activated Macrophage Cell Line: Gene Silencing, Toxicity and Off-Target Gene Expression

Linda B. Jensen • Joscha Griger • Broes Naeye • Amir K. Varkouhi • Koen Raemdonck • Raymond Schiffelers • Twan Lammers • Gert Storm • Stefaan C. de Smedt • Brian S. Sproat • Hanne M. Nielsen • Camilla Foged

Received: 10 June 2011 / Accepted: 13 September 2011 / Published online: 5 October 2011

ABSTRACT

Purpose Tumor necrosis factor α (TNF-α) plays a key role in the progression of rheumatoid arthritis and is an important target for anti-rheumatic therapies. TNF-α expression can be silenced with small interfering RNA (siRNA), but efficacy is dependent on efficient and safe siRNA delivery vehicles. We aimed to identify polymeric nanocarriers for anti-TNF-α siRNA with optimal efficacy and minimal off-target effects *in vitro*.

Methods TNF-α silencing with polymeric siRNA nanocarriers was compared in lipopolysaccharide-activated RAW 264.7 macrophages by real-time reverse transcription (RT)-PCR. Expression of non-target genes involved in inflammation, apoptosis, and cell cycle progression was determined by RT-PCR, toxicity evaluated by propidium iodide and annexin V staining.

Results PAMAM dendrimers (G4 and G7) and dextran nanogels mediated remarkably high concentration-dependent gene silencing and low toxicity; dioleoyltrimethylammoniumpropane-modified poly (DL-lactide-co-glycolide acid) nanoparticles, thiolated, trimethylated chitosan and poly[(2-hydroxypropyl)methacrylamide 1-methyl-2-piperidine methanol] polyplexes were less efficient transfectants. There were minor changes in the regulation of off-target genes, mainly dependent on nanocarrier and siRNA concentration.

Conclusions Dextran nanogels and PAMAM dendrimers mediated high gene silencing with minor toxicity and off-target transcriptional changes and are therefore expected to be suitable siRNA delivery systems *in vivo*.

KEY WORDS delivery · macrophages · polymer · siRNA · TNF-α

ABBREVIATIONS

Act	β-actin
AEMA	2-aminoethyl methacrylate hydrochloride
ANOVA	analysis of variance
Ccna2	cyclin a2
Cdk7	cyclin-dependent kinase 7
CP	crossing point
Cse1L	cellular apoptosis susceptibility protein 1L
DAB	diaminobutane dendrimers

L. B. Jensen • J. Griger • H. M. Nielsen • C. Foged (✉)
Department of Pharmaceutics and Analytical Chemistry
Faculty of Pharmaceutical Sciences, University of Copenhagen
Universitetsparken 2
2100 Copenhagen O, Denmark
e-mail: cfo@farma.ku.dk

B. Naeye • K. Raemdonck • S. C. de Smedt
Laboratory of General Biochemistry and Physical Pharmacy
Ghent University
Harelbekestraat 72
9000 Ghent, Belgium

A. K. Varkouhi • R. Schiffelers • T. Lammers • G. Storm
Department of Pharmaceutics, Faculty of Science, Utrecht University
Sorbonnelaan 16
3584 CA Utrecht, The Netherlands

T. Lammers
Department of Experimental Molecular Imaging
RWTH Aachen University
Pauwelsstrasse 30
52074 Aachen, Germany

B. S. Sproat
Chemconsilium GCV
Jaarmarktstraat 48
2221 Booischot, Belgium

Present Address:
J. Griger
Max Delbrueck Centre for Molecular Medicine
Robert-Roessle-Str. 10
13125 Berlin-Buch, Germany

dex-HEMA	dextran hydroxyethyl methacrylate
dex-MA	dextran methacrylate
DMEM	Dulbecco´s Modified Eagle´s Medium
DOTAP	1,2-dioleoyloxy-3-trimethylammoniumpropane
EE	encapsulation efficiency
EGFP	enhanced green fluorescent protein
FBS	fetal bovine serum
FITC	fluorescein isothiocyanate
G	generation
Gus	β-glucuronidase
HEPES	4-(2-hydroxyethyl)-piperazine-1-ethanesulfonic acid
IL	interleukin
INF	interferon
LPS	lipopolysaccharide
LUC	luciferase
NHS-PEG	N-hydroxysuccinimidyl-activated methoxypolyethylene glycol 5000 propionic acid
N/P	amine-to-phosphate ratio
OAS1d	oligoadenylate Synthetase-Like Protein 1d
OF	oligofectamine
PAMAM	poly(amidoamine)
PCI	photochemical internalization
PDI	polydispersity index
PEG	polyethylene glycol
PEI	polyethylenimine
PF	polyfect (based on PAMAM dendrimers)
pHPMA-MPPM	poly((2-hydroxypropyl)methacrylamide 1-methyl-2-piperidine methanol)
PI	propidium iodide
PLGA	poly(DL-lactide-co-glycolide acid)
PVA	polyvinylalcohol
RA	rheumatoid arthritis
RNAi	RNA interference
RT	reverse transcription
siRNA	small interfering RNA
TLR	toll-like receptor
TMAEMA	[2-(methacryloyloxy)ethyl]-trimethylammonium chloride
TMC-SH	thiolated N,N,N-trimethylated chitosan
TNF-α	tumor necrosis factor α

INTRODUCTION

Rheumatoid arthritis (RA) is a chronic autoimmune disorder, characterized by systemic inflammation of synovial joints leading to erosion and cartilage destruction. It is the most frequently occurring autoimmune disease affecting 0.5–1% of the world's population (1). As its etiology remains unknown, current treatment modalities focus on short-lived pain relief, inflammation control and prevention of joint destruction.

Macrophages are local and systemic amplifiers of RA due to their high abundance in the inflamed synovial membranes (2,3). Macrophages produce proinflammatory cytokines such as tumor necrosis factor-α (TNF-α) and interleukin 1 (IL-1) that play a central role in RA progression by stimulating the production of additional inflammatory mediators and the recruitment of immune cells to the joint (4). Although successful anti-TNF-α biologics have been developed (1,3,4), novel and more long-lived treatment strategies are needed because many patients fail to respond to these drugs or suffer from an increased risk of opportunistic infections such as tuberculosis as a result of the immune-compromising treatment (5). One such strategy is based on RNA interference (RNAi) therapeutics, e.g. small interfering RNA (siRNA) that mediate specific knockdown of TNF-α at the transcriptional level (6–8), and *in vivo* proof-of-concept exists in pre-clinical models (9–12).

The therapeutic use of siRNA is dependent on safe and efficient delivery vectors that can protect against premature degradation and transport the siRNA across membrane barrier(s) to the cytoplasm of target cells, where it can enter the RNA interference pathway (13,14). Several non-viral strategies have been exploited for delivery, including polymeric nanocarriers (15), which can be classified as polyplexes or nanospheres. Polyplexes are formed by self-assembly via electrostatic interaction between cationic polymers and the polyanionic siRNA, and are usually formulated at a high cationic charge density to facilitate binding to anionic proteoglycans present on the cell surfaces (16). Well-known examples are the synthetic polymers polyethylenimine (PEI) (17,18) and poly(amidoamine) (PAMAM) dendrimers (19,20). However, the use of polyplexes is limited by a low colloidal stability under physiological conditions and a risk of accumulation and toxicity in the body upon repeated administration due to their non-biodegradable nature (21,22). Therefore, there is a substantial interest in exploring biodegradable and more stable polymeric carriers (22,23). An example is the biocompatible and biodegradable polysaccharide chitosan, which in recent years has been chemically modified to improve complex stability and transfection properties (24,25).

In contrast, nanospheres are matrix systems, wherein siRNA can be entrapped, offering physical protection against nuclease activity as well as a more favorable colloidal stability as compared to polyplexes. Examples are dextran nanogels (26,27) and poly(DL-lactide-co-glycolide acid) (PLGA) based nanoparticles (28), which represent a controllable and alterable matrix degradation profile to extend the release of siRNA, which is important for obtaining long-term RNAi effects.

A drawback of polymer-based siRNA delivery is the potential risk of inducing unintended side effects caused by i) the siRNA, ii) the nanocarrier or iii) the siRNA-loaded nanocarrier. The siRNA molecules can trigger the innate immune system via recognition by Toll-like receptors (TLRs) 3, 7 and 8, which are predominantly located in the endosomal compartments, resulting in the induction of high levels of cytokines, in particular TNF-α and interferon-α (INF-α), and may lead to toxicity (29,30). Many particulate delivery systems are internalized by cells via endocytosis and serve to localize siRNA in close vicinity to the TLRs, which may amplify the innate response. This recognition can to some degree be minimized or even avoided by e.g. chemical siRNA modifications, in particular 2′-O-methylation of the sense strand (31). In addition, the nanocarrier by itself can engage the stimulation of immune receptors (32), and as a further complication, the adverse effects seem to be dependent on factors such as cell type, route of administration and siRNA sequence and structure (30).

In recent years, an increasing number of studies have addressed the effects of nanocarrier-mediated gene delivery on off-target genes by e.g. microarray analysis (13,29,33,34). For siRNA delivery in particular, the commercial Polyfect® (PF) transfection reagent based on PAMAM dendrimers was shown to affect the expression of more than 1000 genes (35), while siRNA-complexed carbosilane dendrimers influenced the expression of more than 11,000 genes in human primary macrophages, which was more than two-fold higher than the number of deregulated genes caused by the carrier alone (36). These microarray analyses generally suggest alterations in the expression patterns of genes involved in apoptosis, cell growth/maintenance and inflammatory responses. However, a direct comparison between the different studies is often not possible due to differences in cell line, exposure time and siRNA sequence. Therefore direct comparative studies of different types of nanocarriers are lacking in the literature.

Here, we present a direct *in vitro* comparison of a selected panel of promising polyplexes and nanospheres, which have previously been shown to mediate siRNA delivery (Table I). The murine macrophage cell line RAW 264.7 was selected for the studies because TNF-α silencing has been successfully achieved in this cell line with the commercially available *in vitro* transfection reagent Trans-IT TKO (Mirus Corp) (37,38). Specific TNF-α knockdown was evaluated in the lipopolysaccharide (LPS) stimulated cell line, and toxicity was assessed by annexin V/propidium iodide (PI) staining. Additionally, the transcriptional level of five off-target genes was evaluated by real time reverse transcription (RT) PCR to investigate the potential adverse effects of the nanocarrier-mediated siRNA delivery (Table II).

MATERIALS AND METHODS

Materials

2′-O-Methyl modified dicer substrate asymmetric siRNA duplexes directed against TNF-α and a negative control sequence were provided by Integrated DNA Technologies Inc. (IDT, Coralville, IA, USA) as dried, purified and desalted duplexes, and re-annealed as recommended by the supplier in the IDT duplex buffer consisting of 30 mM 4-(2-hydroxyethyl)-piperazine-1-ethanesulfonic acid (HEPES) and 100 mM potassium acetate, pH 7.5. The siRNAs had the following sequences and modification patterns:

TNF-α sense 5'-pGUCUCAGCCUCUUCUCAUUC CUGct-3', antisense
5'-AGCAGGAAUGAGAAGAGGCUGAGACAU-3',
and negative control sense
5'-pCGUUAAUCGCGUAUAAUACGCGUat-3' and antisense
5'-pAUACGCGUAUUACGCGAUUAACGAC-3'

where lower case letters represent deoxyribonucleotides, underlined capital letters represent 2′-O-methylribonucleotides and p represents a phosphate residue. Amine-terminated PAMAM G4 and G7 dendrimers with an ethylenediamine core, hydroxysuccinimidyl-activated methoxypolyethylene glycol 5000 propionic acid solution (NHS-PEG), penicillin, streptomycin, L-glutamine and LPS (γ-irradiated, <1% protein) were obtained from Sigma-Aldrich (St. Louis, MO, USA), and PLGA (lactide:glycolide molar ratio 75:25, Mw: 20 kDa) was purchased from Wako Pure Chemical Industries (Osaka, Japan). Polyvinylalcohol (PVA) 403 with an 80.0% degree of hydrolysis was provided by Kuraray (Osaka, Japan), and 1,2-dioleoyloxy-3-trimethylammoniumpropane (DOTAP) was purchased from Avanti Polar Lipids (Alabaster, AL, USA). Primers were supplied by TAG Copenhagen (Copenhagen, Denmark) and HEPES buffer pH 7.4 was from AppliChem (Darmstadt, Germany). Sterilized Milli-Q water was used for buffer dilutions, and buffers were filtered through 0.2 μm filters (Millipore, Carrigtwohill, Ireland) prior to use. For RNA, cDNA and primer dilutions, PCR grade water was used (Roche, Basel, Switzerland). All chemicals were obtained commercially at analytical grade and used as received.

Preparation of Polyplexes

All polyplex formulations were prepared at a nitrogen-to-phosphate (N/P) ratio of 12 in 5 mM HEPES buffer, pH 7.4. pHPMA-MPPM (Mw: 240 kDa, polydispersity index (PDI): 1.65) and TMC-SH (Mw: 144 kDa, PDI: 2.4, 7.0% degree of thiolation were synthesized, purified and formulated with siRNA into polyplexes as described

Table I Polymeric Nanocarrier Systems Examined in the Current Study

Carrier	Description	Modification	siRNA silencing effect *in vitro*	siRNA release mechanism
PAMAM dendrimers G4 and G7	Synthetic, mono-disperse, non-biodegradable cationic polymers for electrostatic siRNA complexation.	None (purchased with ethylenediamine core).	20 and 45% silencing in J-774-EGFP cells with G4 and G7 at 50 nM siRNA after 72 h transfection (first 5 h with complex) (19).	Polyplex dissociation.
TMC-SH	Biodegradable cationic polymer for electrostatic siRNA complexation (25).	Improved polymer solubility by methylation and 7% thiolation is likely to increase extracellular stability (25,40,42).	45 and 60–80% silencing with and without serum in H1299-LUC cells at 160 nM siRNA and 48 h transfection (first 24 with complex) (42).	Polyplex dissociation.
pHPMA-MPPM	Biodegradable cationic polymer for electrostatic siRNA complexation (41).	Contains a hydrolysis-sensitive biodegradable linker with increased stability at pH 5 to protect the siRNA in the endosomal compartment (39,41).	70 and 45% silencing with and without PCI in H1299-LUC cells at 80 nM siRNA and 48 h transfection (first 4 h with complex) (39).	Polyplex dissociation upon degradation of the linker.
Dextran nanogels (dex-HEMA-*co*-TMAEMA)	Polymeric matrix system with a three-dimensional polymer network for siRNA entrapment (26).	Suitable for siRNA delivery due to high siRNA loading and cytosol delivery of intact siRNA (26,27).	85 and 70% silencing with and without PCI in HuH-7-LUC cells at 250 nM siRNA and 48 h transfection (first 4 h with complex) (27). Additionally >80% silencing has been achieved with 100 nM siRNA and 72 h transfection (unpublished results)	Degradation of nanogels and dissociation of the siRNA.
PEGylated dextran nanogels (dex-MA-*co*-AEMA-*co*-TMAEMA)	Modified dextran nanogels with a PEG coating (44).	PEGylated to improve serum stability.	80% silencing in Huh-7-EGFP cells at 250 nM siRNA and 72 h transfection (4 h with nanogels) (44).	Degradation of nanogels and dissociation of the siRNA.
PLGA nanoparticles	FDA approved biodegradable polymeric matrix system (28).	Modification of the matrix with 15% cationic lipid (DOTAP) resulting in a cationic surface charge.	54% silencing in H1299-EGFP cells at 100 nM siRNA and 48 h transfection (all with complex) (45).	Hydrolysis of the PLGA matrix and dissociation of the siRNA.

previously (39–42). Commercial PAMAM dendrimers were used as received without further purification and formulated into siRNA-containing dendriplexes as reported recently (43). Briefly, equal volumes of siRNA and polymer solutions were mixed by adding the siRNA solution dropwise to the polymer solution, followed by at least 10 s of immediate vortex mixing. The mixture was left at room temperature for 30 min for dendrimers and pHPMA-MPPM and for 3 h for TMC-SH to allow complex formation. TMC-SH was dissolved immediately before complexation, while pHPMA-MPPM was dissolved over 3 days in HEPES buffer at pH 5. The following polymer and siRNA concentrations and volumes were used: 435 and 189.7 μg/ml for TMC-SH and pHPMA-MPPM, respectively, where 750 μl polymer solution was mixed with an equal volume of 40 μg/ml siRNA solution, resulting in a final siRNA concentration of 1.19 and 1.14 μM siRNA for TNF-α and negative control siRNAs, respectively. For the dendrimers, 50 μl of 10 μM siRNA solution was added to an equal volume of 97.6 and 12.2 μM PAMAM G4 and G7, respectively, and following complexation, further dilution to a total volume of 417 μl was performed, resulting in a final siRNA concentration of 1.2 μM.

Preparation of siRNA-Loaded Dextran Nanogels

Dextran nanogels were prepared as described previously (27,44) and redispersed in 5 mM HEPES buffer, pH 7.4. Briefly, dextran nanogels prepared by the inverse miniemulsion photopolymerization method were cationized by co-crosslinking [2-(methacryloyloxy)ethyl]-trimethyl-ammonium chloride (TMAEMA) monomers with the degradable dextran hydroxyethyl methacrylate (dex-HEMA). Nanogels with primary amine functional groups for PEGylation were prepared by co-crosslinking 2-aminoethyl methacrylate hydrochloride (AEMA), TMAEMA and dextran methacrylate (dex-MA). During the preparation of dextran nanogels, several washing steps were used to remove non cross-linked components (27,44). ^{1}H-NMR on the degradation products of the nanogels has shown that this is indeed the case. No traces of photo-initiator, surfactants or organic solvents could

Table II Gene Targets Evaluated for Transcriptional Changes Upon siRNA Delivery, Including a Description of the Protein Function, and Previous Observations from Transcriptional Analyses of Carrier Systems

Gene	Protein function	Previous observations from microarrays
Interleukin-1β (Il-1β)	Produced by activated macrophages and mediates an inflammatory response. Is involved in a variety of cellular activities, including cell proliferation, differentiation and apoptosis.	Progressive release has been observed in mice after administration of glycosylated PAMAM dendrimers (65) and gene up regulation was observed in human macrophages after administrating cabosilane dendrimers with and without siRNA (36).
Cd14 antigen precursor (Cd14)	Surface antigen important for LPS activation as it cooperates with MD-2 and TLR4 to mediate an innate immune response to LPS, leading to NF-κB activation, cytokine secretion and the inflammatory response. Up-regulates cell surface molecules, including adhesion molecules.	Up-regulated by the DAB16 dendrimers in human alveolar epithelial A549 cells, but not by polyfect (PF) or oligofectamine (OF) (50).
Cellular apoptosis susceptibility protein 1L (Cse1L)	Analogue to the yeast chromosome segregation 1-like gene. Plays an important role in regulating cancer cell proliferation and apoptosis, where up regulation is correlated with a worsened patient outcome (66).	Down-regulated by DAB16 dendrimers and PF, but up-regulated by OF in human alveolar epithelial A549 cells (50).
Cyclin-dependent kinase 7 (Cdk7)	Cdks are activated by the binding to a cyclin protein and mediate the progression of the cell cycle. Involved in cell cycle control and in RNA polymerase II-dependent transcription. Its expression and activity is constant throughout the cell cycle.	Down-regulated by PF but not by OF or DAB16 dendrimers in human alveolar epithelial A549 cells (50).
Cyclin a2 (Ccna2)	Essential for the control of the cell cycle at the G1/S (start) and the G2/M (mitosis) transitions.	Down-regulated by OF but not by PF or DAB16 dendrimers in human alveolar epithelial A549 cells (50).

be detected. Both types of nanogel formulations were loaded with siRNA by adding 400 µl of a 10 µM siRNA solution to an equal volume of a nanogel dispersion (2 mg/ml). Subsequently, either 400 µl of HEPES buffer or a freshly prepared 10 mg/ml NHS-PEG was added and incubated for 1 h at 4°C to generate siRNA-loaded non-PEGylated (dex-HEMA) and PEGylated (dex-MA) nanogels, respectively. The final siRNA concentration was 3.33 µM. For the PEGylated dextran nanogels, no purification step was applied to remove unreacted PEG. Although dialysis can remove the latter, the amount of NHS-PEG added is carefully chosen to ensure the optimal balance between sufficient PEGylation and an excess of NHS-PEG.

Preparation of DOTAP-Modified PLGA Nanoparticles

DOTAP-modified PLGA nanoparticles (also called DOTAP/PLGA nanoparticles below) were produced by the double emulsion solvent evaporation method as reported previously (45). In brief, 125 µl of either 120.3 µM TNF-α siRNA or 105.1 µM negative control siRNA in TE-buffer (10 mM Tris-HCl, 1 mM EDTA, pH 7.5; Invitrogen, Paisley, United Kindom) was emulsified with 250 µl of a DOTAP/PLGA (15:85, w/w) binary mixture in chloroform with a total concentration of DOTAP and PLGA of 60 mg/ml. The mixture was sonicated for 90 s using a high-intensity sonicator (MISONIX Sonicator 4000, Qsonica LLC, Newtown, CT, USA) to obtain a water-in-oil (w/o) emulsion. A volume of 1 ml 2% (w/v) PVA in water was added to the emulsion, and a second sonication step of 60 s was performed, resulting in a water-in-oil-in-water (w/o/w) double emulsion. The double emulsion was subsequently diluted with 5 ml of 2% (w/v) PVA in water and left under agitation overnight to allow for evaporation of residual chloroform. The nanoparticles were isolated by centrifugation for 12 min at 4°C and 18,000 × *g*. The supernatant was discarded, and the pellet containing the nanoparticles was re-dispersed in diethyl pyrocarbonate-treated water. Centrifugation and re-dispersion of the nanoparticle pellet was repeated three times to ensure the complete removal of the PVA. The siRNA encapsulation efficiency was determined as described previously (28).

Particle Size, Polydispersity Index (PDI) and Zeta Potential

The particle size distribution and PDI of the nanocarriers were determined by dynamic light scattering, and the surface charge was estimated by zeta potential analysis (laser-Doppler electrophoresis). For polyplexes and nanogels, particle size measurements were performed on undiluted samples, while the zeta potential measurements where done on samples diluted two-fold in HEPES buffer. For DOTAP/PLGA nanoparticles, approximately 0.15 mg/ml PLGA was used

for measurements. The measurements were repeated three times per sample ($n=1$) and were performed using a Zetasizer Nano ZS (Malvern Instruments, Worcestershire, United Kingdom) equipped with a 633 nm laser and 173° detection optics. Malvern DTS v.6.10 software (Malvern Instruments) was used for data acquisition and analysis, and a Nanosphere™ Size Standard (220±6 nm, Duke Scientific Corporation, Palo Alto, CA, USA) and a zeta potential transfer standard (−50±5 mV, Malvern Instruments) were used to verify the performance of the instrument. For viscosity and refractive index, the values of pure water were used.

Pyrogen Test

An *in vitro* granulocyte assay was used to test for the presence of pyrogens in the formulations (46). Polymer concentrations corresponding to the highest concentrations tested in the *in vitro* transfection experiments were used (polymer concentration at 100 nM siRNA).

Cell Culture

The murine macrophage cell line RAW264.7 was purchased from American Type Culture Collection (TIB71) at an unspecified passage number. The cells were maintained in Dulbecco´s Modified Eagle´s Medium (DMEM) (Aldrich, St. Louis, MO, USA) supplemented with 100 U/ml penicillin, 100 μg/ml streptomycin, 2 mM L-glutamine and 10% (v/v) fetal bovine serum (PAA Laboratories, Pasching, Austria), which will be referred to as complete medium in the text below. The cells were grown in an atmosphere of 5% CO_2/95% O_2 at 37°C changing the growth medium three times a week and sub-cultured approximately 1:10 twice a week by detaching the cells from the culture flask by scraping. The cells were sub-cultured at least five times before used in transfection assays, and used before reaching passage 12.

Cell Transfection and Harvesting

The siRNA-loaded nanocarriers were diluted to a total volume of 100 μl with DMEM to a concentration of 25, 50 and 100 nM siRNA in the final cell culture medium. As control, 6 μl of the cationic polymer/lipid transfection agent Trans-IT TKO (Mirus Corp., Madison, WI, USA) was used with 2.5 to 100 nM siRNA. The transfection mixture was added to 12-well tissue culture plates in triplicates, followed by addition of approximately 5×10^5 freshly harvested RAW 264.7 cells in 500 μl of complete medium. Transfections were performed for 24 h in 5% CO_2/95% O_2 at 37°C, and 3 h prior to harvesting, 100 μl complete medium containing LPS was added to a final concentration of 5 ng/ml. Prior to harvesting, 1 ml of cold phosphate-buffered saline was added, and the cells were loosened with a pipette.

RNA Purification and cDNA Synthesis

RNA was isolated using the NucleoSpin RNA II kit (Macherey-Nagel GmbH & Co, Düren, Germany) according to the manufacturer´s instructions. The total RNA levels in the samples were quantified using the Nanodrop 2000 C Spectrophotometer (NanoDrop Technologies, Inc., Wilmington, DE, USA), and reverse transcription of 1 μg total RNA was performed with a mix of oligo dT and random hexamer primers applying the iScript cDNA synthesis Kit (Bio-Rad Laboratories, (Hercules, CA, USA). The cDNA was diluted 1:10 in PCR-grade water and stored at −20°C until further use. All RNA samples displayed a 260/280 ratio between 2.0–2.16.

Real-Time RT-PCR

The specific siRNA knockdown of TNF-α mRNA was evaluated by real time RT-PCR. The PCR reaction was performed in duplicate applying the LightCycler® 480 system (Roche, Basel, Switzerland) in a total reaction volume of 20 μl using 10 μl of the LightCycler® 480 SYBR Green I Master (Roche, Basel, Switzerland), 0.5 μM of forward and reverse primers (except for β-glucuronidase (Gus) where 1 μM was used) (Table III) and 5 μl of 1:10 diluted cDNA. The cycling conditions were as follows: An initial denaturation step at 95°C for 5 min, followed by 35 cycles of denaturation at 95°C for 10 s, annealing at 60°C for 10 s, elongation at 72°C for 10 s. The cycles were followed by a melting curve analysis at 95°C for 5 s, 65°C for 1 min and continuous detection every 5°C until reaching 97°C. The LightCycler® 480 software v 1.5.0 (Roche) was used for crossing point (CP) analysis and normalized according to the average of the two reference genes [Gus and β-actin (Act)], followed by quantification relative to the LPS-treated cells using the comparative ΔΔCP method (47). ΔCP values above 0.3 of the duplicate analysis were excluded from further analysis to ensure reproducibility. Finally, the specific TNF-α knockdown was calculated relative to the negative control siRNA.

Toxicity

The cells were analyzed for annexin V binding and PI incorporation to determine the number of viable and early apoptotic cells. As for the gene silencing, cells were harvested 24 h post-transfection with 3 h LPS incubation, and analysis was performed following the procedure recommended by the supplier, using the FITC-labeled annexin V apoptosis detection kit I (BD, Franklin Lakes, NJ, USA) with minor modifications. Briefly, approximately

Table III Primer Sequences Used for the Real-Time RT-PCR Analyses

Target	Primer sequences	
	Forward	Reverse
Act	5′- CAGCTTCTTTGCAGCTCCTT-3′	5′- CACGATGGAGGGGAATACAG-3′
Gus	5′- AGTTGTGTGGGTGAATGGGA-3	5′- GGAAGGGTATGAGGGGTCAG-3′
TNF-α	5′ - TGCCTATGTCTCAGCCTCTTC-3′	5′- GGTCTGGGCCATAGAACTGA-3′
Il-1β	5′- GCAGCTGGAGAGTGTGGATCCCAA-3′	5′- GGAAGACAGGCTTGTGCTCTGCT-3′
Cd14	5′- CTACCGACCATGGAGCGTGTGCT-3′	5′- CACATCTGCCGCCCCCAAACAA-3′
Cse1L	5′- CTTGTCCTGGAAGGGTTCCCTCGA-3′	5′- AACCATCCTCAGCCGCTGCATG-3′
Cdk7	5′- GGTGTGGGAGTAGACATGTGGGC-3′	5′- AGACTACACATGTCAGGCCACTGC-3′
Ccna2	5′- CTCAGCCCTGCTCTCGCTGCAT-3′	5′- GGAGCAACCCGTCGAGTCTTGAGC-3′

2×10^5 cells were washed twice in cold PBS, resuspended in 100 µl binding buffer and stained with 5 µl of annexin V (concentration not specified) and 5 µl PI (50 µg/µL) solution for 15 min. The cells were analyzed on a FACScan flow cytometer using the CellQuest Software (Becton Dickinson and Company, Franklin Lakes, NJ, USA).

Statistics

Statistical analyses were performed by one-way analysis of variance (ANOVA) at a 0.05 significance level followed by Dunnett's multiple comparison test using SigmaPlot v. 11.0 (Systat Software Inc., San Jose, CA, USA).

RESULTS

TNF-α expression was induced in the murine macrophage cell line RAW264.7 upon TLR-4 dependent activation of the cells with LPS (38,48), which resulted in a more than 15-fold induction of the mRNA expression level (data not shown). A reverse transfection protocol was used, where cells in suspension were added to nanocarrier suspensions to allow for maximal interaction between the cells and the siRNA-nanocarrier complexes (49), and transcriptional gene silencing was evaluated after 24 h incubation. The reverse transfection protocol was optimized with respect to incubation time with LPS and the positive control Trans-IT-TKO tranfection reagent, and quantification of TNF-α transcripts was performed by real time RT-PCR. The TNF-α expression level was normalized to the average level of the two housekeeping genes Act and Gus, which were expressed at high and low levels, compared to the additional panel of genes. Both housekeeping genes displayed very little changes in gene expression levels under the applied experimental conditions (data not shown). This was followed by a normalization to the LPS-induced, non-treated cells by the ΔΔCP method (47), and the specific TNF-α silencing was evaluated from the relative difference in the expression level between the carriers containing TNF-α and negative control siRNA. The Trans-IT-TKO transfection reagent induced a dose-dependent silencing reaching a level of 90% knockdown at 50 nM siRNA (Fig. 1).

Physicochemical Characterization of the Nanocarrier Systems

The nanosphere and polyplex sizes ranged between 100 and 260 nm with relatively low PDIs (Table IV), and only the TMC-SH and the pHPMA-MPPM polyplexes displayed PDIs well above 0.2, where previous investigations have demonstrated PDIs≤0.3 (39,42). A positive zeta potential was observed for all nanocarrier formulations, indicating an overall positive surface charge. The PEG-

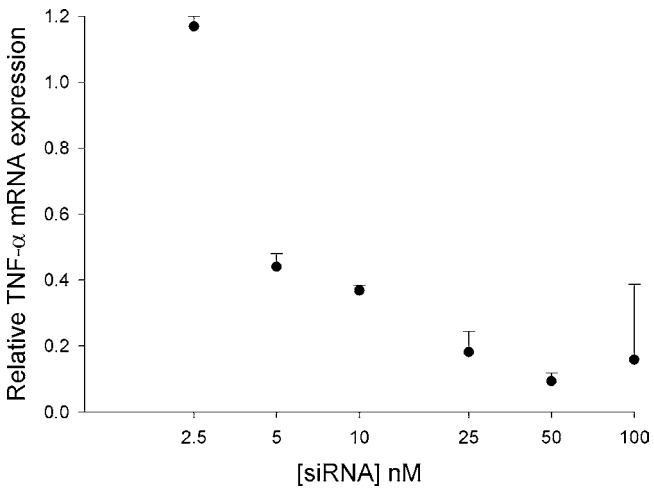

Fig. 1 Dose-response curve for TNF-α silencing in RAW 264.7 cells with the Trans-IT TKO transfection reagent. Results are normalized to non-transfected, LPS-treated cells and denote the TNF-α mRNA expression relative to mRNA levels for the cells transfected with negative control siRNA, which were similar to the expression levels for LPS-treated, non-transfected cells. Results represent the means ± SD of triplicate samples.

Table IV Physicochemical Characteristics of Nanocarriers Loaded with TNF-α and Negative Control siRNA. The Values Reflect Single Measurements of Formulations with TNF-α and Negative Control siRNA (Separated by /)

Polymer	Z-average (nm)	PDI	Zeta potential (mV)
PAMAM G4	190.6 / 204.2	0.039 / 0.055	33.6 / 37.1
PAMAM G7	111.4 / 107.7	0.174 / 0.162	38.1 / 37.8
TMC-SH	116.4 / 110.0	0.320 / 0.359	17.4 / 20.9
pHPMA-MPPM	238.2 / 228.3	0.301 / 0.303	27.4 / 30.2
Nanogel	193.2 / n.d.[a]	0.176 / n.d.[a]	17.1 / n.d.[a]
PEGylated nanogel	189.9 / 190.6	0.208 / 0.215	10.1 / 8.7
DOTAP/PLGA	259.4 / 255.6	0.127 / 0.136	25.7 / 35.2

[a] Not determined

ylated nanogels displayed the lowest zeta potential (8.7 and 10.1 mV) due to a charge shielding effect caused by the PEG (44), while PAMAM dendrimers and pHPMA-MPPM possessed the highest positive zeta potential, suggesting a larger excess of positive surface charge as compared to the other nanocarriers, even though all polyplexes were formulated at an N/P ratio of 12 (Table IV). Finally, the nanocarriers did not interfere with the granulocyte assay as evaluated by spike recovery, and were therefore considered as pyrogen free (data not shown).

TNF-α Gene Silencing

The nanocarrier formulations were tested at three different siRNA concentrations (Fig. 2). All formulations induced a concentration-dependent, sequence-specific gene silencing, and the highest efficiency was obtained with the PEGylated nanogels, PAMAM G4, non-PEGylated nanogels and PAMAM G7 at 100 nM siRNA, showing 75±3%, 85±4%, 90±2% and 96±2% gene silencing, respectively. Even at 25 nM siRNA, a specific knockdown of 57±3% and 60±4% was observed for the nanogels and PAMAM G7, respectively, which reached the same silencing level as the Trans-IT-TKO positive control transfection reagent, even though higher concentrations of siRNA were required (Figs. 1 and 2). For comparison, 27.5±23%, 39.1±7% and 41±3% silencing was obtained with the pHPMA-MPPM, DOTAP/PLGA and TMC-SH nanocarriers, while a specific knockdown of 30±9% was observed with the naked siRNA at 100 nM (Fig. 2), showing equal effect of transfection with naked siRNA and the pHPMA-MPPM and DOTAP/PLGA nanocarriers ($p>0.05$). The silencing mediated by naked siRNA might be related to damage of the cell membranes upon harvesting, as the siRNA (± carrier) is mixed with cells immediately after harvesting (49).

Toxicity

PI and Annexin V staining combined with flow cytometry was used to estimate the fraction of non-viable cells characterized by membrane permeabilization resulting in DNA intercalation of PI, and cells in early apoptosis from the degree of translocation of the membrane phospholipid phosphatidylserine from the inner to the outer membrane leaflet (recognized by annexin V). This was done in order to distinguish the fraction of cells undergoing early apoptosis from the population of viable cells (Fig. 3). For the low concentration of siRNA, none of the carriers displayed any significant toxicity, and the PAMAM G4 dendriplexes were well-tolerated in the entire concentration range investigated ($p>0.05$). Transfection with PAMAM G7 dendrimers resulted in a decreased percentage of viable cells to between 85–90%, with no apparent effect of the concentration,

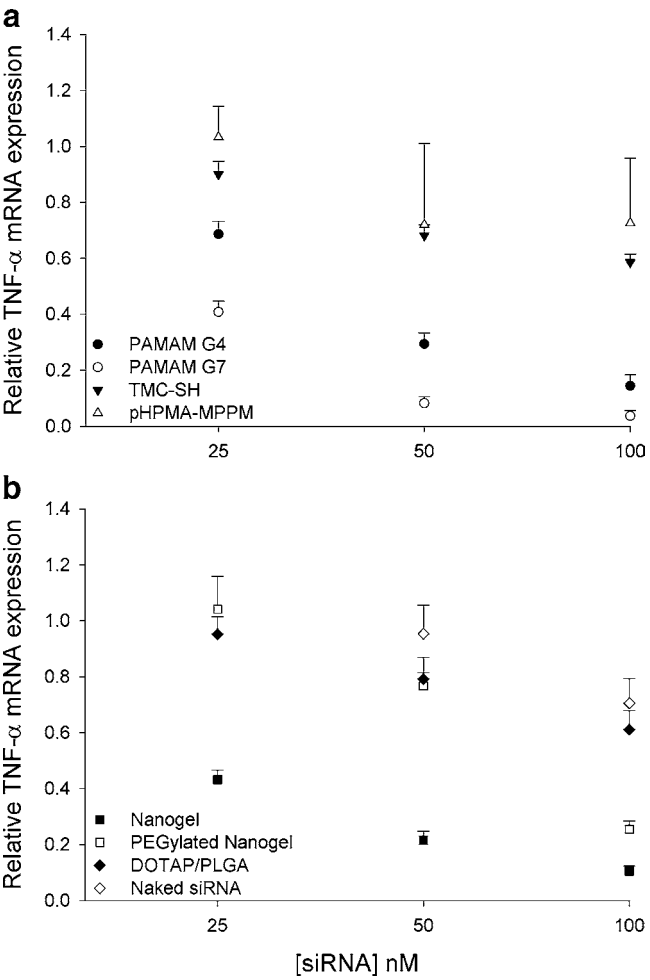

Fig. 2 Nanocarrier-mediated TNF-α silencing in RAW 264.7 cells. Normalization to LPS-treated cells without siRNA was performed, and results denote the TNF-α mRNA expression relative to transfection with negative control siRNA. (**a**) Polyplexes, (**b**) nanospheres with inclusion of naked siRNA at a concentration of 50 and 100 nM. Results denote the means ± SD of triplicate samples.

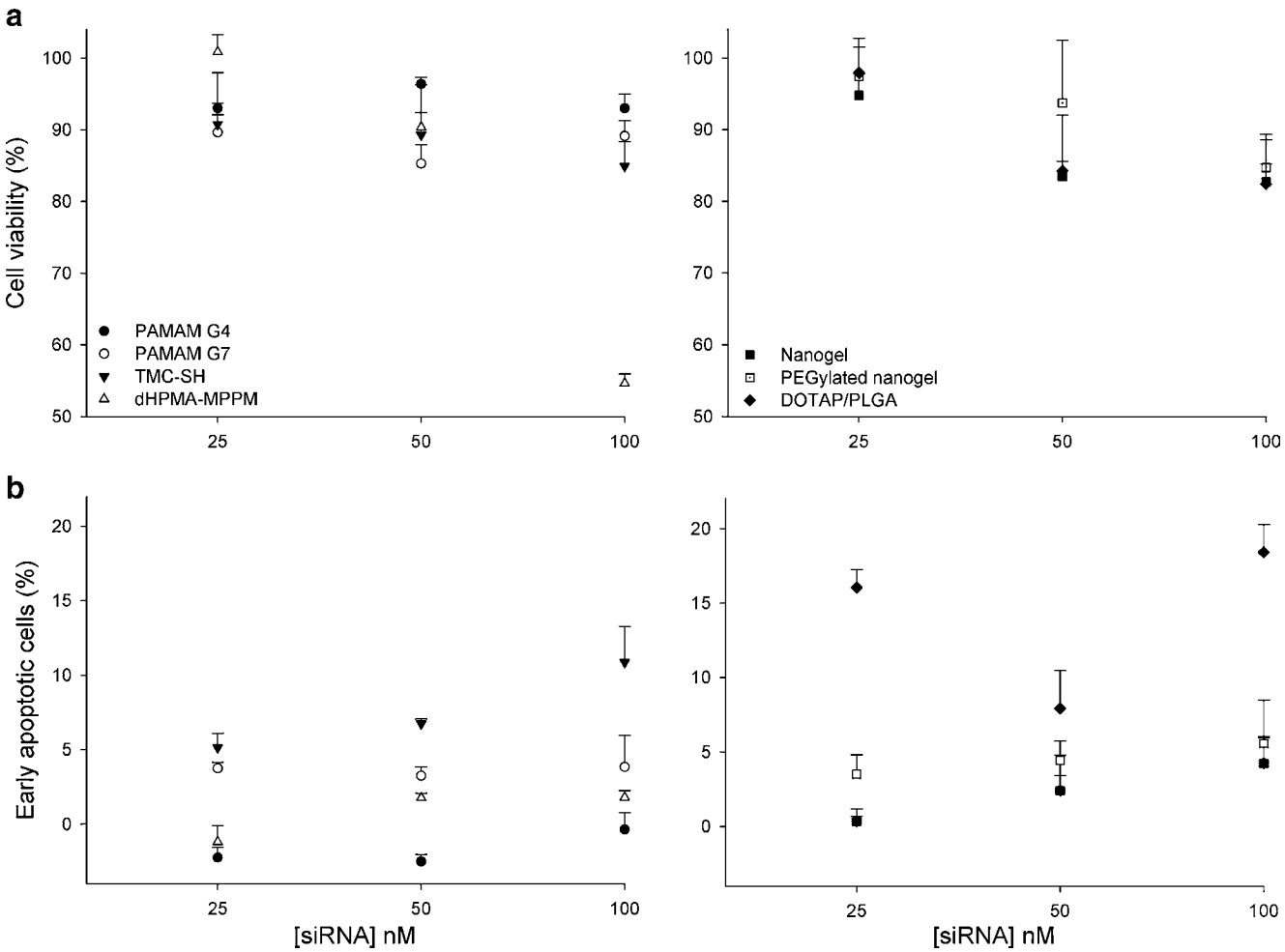

Fig. 3 Viability of cells treated with nanocarriers upon TNF-α silencing in RAW 264.7 cells, including cells in early apoptosis. Viable cells were defined as negative for PI staining, and within the fraction of viable cells, the early apoptotic cells were identified by annexin V staining. (**a**) Viability, (**b**) early apoptotic cells, where polyplexes and nanospheres are depicted to the left and right, respectively. Nontransfected cells treated with LPS were used for background subtraction. Results denote the means ± SD of triplicate samples.

while the reduced viability caused by TMC-SH, nanogel, PEGylated nanogel, DOTAP/PLGA and pHPMA-MPPM was concentration-dependent (Fig. 3a). The highest toxicity was observed for the latter at 100 nM siRNA, displaying 54±1.3% viable cells, showing a drastic increase in toxicity when the concentration of the siRNA-loaded nanocarrier complex was increased from 50 to 100 nM siRNA. For comparison, the cells tranfected with the Trans-IT TKO control transfection reagent displayed 73±7% viability (data not shown).

The highest percentage of cells undergoing early apoptosis was observed for the DOTAP/PLGA and the TMC-SH treated cells. A dose-dependent induction of apoptosis was apparent for the TMC-SH as well as the nanogels and PEGylated nanogels, while DOTAP/PLGA nanoparticles and PAMAM G7 induced similar levels of apoptosis in the entire detection range ($p<0.05$) (Fig. 3b). However, all delivery systems were rather well-tolerated in the investigated concentration range, as the majority of the nanocarriers only reduced the viability with a maximum of 15% compared to the non-transfected cells and with less than 5% cells undergoing early apoptosis (Fig. 3).

Nanocarrier-Dependent Changes in Gene Expression

The nanocarriers loaded with siRNA were compared further to evaluate if they induced changes in the expression level of a panel of five selected non-targeted genes (Table II). The cells were transfected with siRNA-loaded nanocarriers for 24 h and activated with LPS, which was added to the cell cultures 3 h prior to harvesting, and the gene expression levels were measured relative to the level in LPS-activated, non-transfected cells after normalization to the average of the two housekeeping genes (Act and Gus). The values for the expression levels including standard deviations and statistics are given in Table V. The

Table V Values for the Relative Gene Expression of Il-1β, Cd14, Cse1L, Cdk7 and Ccna2 after Treatment with Nanocarriers Loaded with TNF-α siRNA at Three Different siRNA Concentrations. Data has been Normalized to the Levels for LPS-treated Cells Without siRNA. The Green and Red Labels Indicate Significant Changed Expression Level ($p < 0.05$), Compared to the LPS-treated Cells. Results Denote the means ±SD of Triplicate Samples

	Il1β	Cd14	Cse1l	Ccna2	Cdk7
DOTAP/PLGA 25 nM	0.696 ± 0.101	0.877 ± 0.048	1.309 ± 0.083	1.262 ± 0.060	1.044 ± 0.054
DOTAP/PLGA 50 nM	0.405 ± 0.029	0.936 ± 0.063	1.016 ± 0.095	1.184 ± 0.106	0.891 ± 0.072
DOTAP/PLGA 100 nM	0.341 ± 0.007	0.895 ± 0.018	1.095 ± 0.073	1.079 ± 0.035	0.901 ± 0.044
Nanogel 25 nM	1.149 ± 0.082	1.012 ± 0.033	1.338 ± 0.203	1.088 ± 0.022	1.330 ± 0.083
Nanogel 50 nM	1.269 ± 0.127	0.949 ± 0.126	1.367 ± 0.011	1.289 ± 0.079	1.384 ± 0.153
Nanogel 100 nM	0.517 ± 0.239	0.793 ± 0.041	1.070 ± 0.132	1.222 ± 0.016	1.235 ± 0.313
PEG-Nanogel 25 nM	0.895 ± 0.191	1.097 ± 0.14	1.176 ± 0.039	1.231 ± 0.045	1.208 ± 0.155
PEG-Nanogel 50 nM	0.833 ± 0.053	0.983 ± 0.041	1.010 ± 0.105	1.087 ± 0.069	1.051 ± 0.132
PEG-Nanogel 100 nM	1.305 ± 0.101	0.924 ± 0.075	1.652 ± 0.033	1.170 ± 0.022	1.447 ± 0.193
PAMAM G4 25 nM	1.007 ± 0.057	1.215 ± 0.099	1.146 ± 0.074	1.078 ± 0.031	1.265 ± 0.074
PAMAM G4 50 nM	0.803 ± 0.038	1.046 ± 0.064	1.128 ± 0.097	1.514 ± 0.415	1.257 ± 0.066
PAMAM G4 100 nM	0.607 ± 0.062	0.972 ± 0.058	0.963 ± 0.019	1.017 ± 0.033	1.075 ± 0.054
PAMAM G7 25 nM	0.947 ± 0.164	1.191 ± 0.099	1.241 ± 0.213	0.882 ± 0.043	1.362 ± 0.201
PAMAM G7 50 nM	0.944 ± 0.159	1.126 ± 0.121	1.246 ± 0.230	1.152 ± 0.122	1.478 ± 0.302
PAMAM G7 100 nM	0.985 ± 0.313	1.099 ± 0.064	1.746 ± 0.403	1.368 ± 0.426	2.246 ± 0.547
TMC-SH 25 nM	1.224 ± 0.094	0.965 ± 0.011	1.341 ± 0.128	1.106 ± 0.109	1.453 ± 0.201
TMC-SH 50 nM	1.020 ± 0.139	0.911 ± 0.063	1.266 ± 0.117	1.095 ± 0.065	1.377 ± 0.153
TMC-SH 100 nM	0.818 ± 0.030	0.806 ± 0.045	1.101 ± 0.055	1.025 ± 0.019	1.150 ± 0.078
pHPMA-MPPM 25 nM	0.458 ± 0.069	0.884 ± 0.084	1.014 ± 0.106	0.919 ± 0.065	0.999 ± 0.086
pHPMA-MPPM 50 nM	0.333 ± 0.014	0.702 ± 0.025	0.766 ± 0.057	0.785 ± 0.068	0.747 ± 0.068
pHPMA-MPPM 100 nM	0.408 ± 0.033	0.709 ± 0.082	0.889 ± 0.027	0.619 ± 0.021	0.930 ± 0.063

expression levels were also measured in cells transfected with negative control siRNA at the three siRNA concentration levels, but the values have for simplicity not been included in Table V since all values were in the same range.

The cytokine IL-1β is like TNF-α an important mediator of the innate immune system, enhancing inflammation and bone destruction during RA, and is produced by activated macrophages, also upon induction with LPS (3). The PAMAM G4, TMC-SH and DOTAP-modified PLGA nanocarriers displayed a dose-dependent down-regulation of Il-1β gene expression, while a significant up-regulation was observed only for the PEGylated nanogels at the highest concentration (Table V). These data therefore suggest that some of the polymers reduce inflammatory signaling by down-regulating Il-1β gene expression.

The three genes Cd14 (CD14 antigen precursor), Cse1l (cellular apoptosis susceptibility protein 1L) and Cdk7 (cyclin-dependent kinase 7) were included in the analysis because they have been shown to be deregulated upon 4 h incubation with 20 mg/ml of PF (polyfect) transfection reagent (based on PAMAM dendrimers) and diaminobutane dendrimers with 16 primary amines (DAB16) (50). In addition, Ccna2 (cyclin a2) was included, since this gene displayed no change in expression upon incubation with the dendrimers, but down-regulated expression upon treatment with the lipid-based transfection reagent oligofectamine (OF) (50). For comparison, in the current study a concentration of 14 mg/ml of PAMAM G4 and G7 dendrimers in formulation with siRNA (at 100 nM) was applied, which is in a range comparable to the concentration used for the microarray analysis. All four genes were significantly deregulated upon siRNA nanocarrier application (Table V), but only Cdk7 displayed a more than 2-fold up-regulation in gene expression, which was observed upon treatment with 100 nM siRNA complexes with PAMAM G7. The observed changes in expression levels are therefore rather modest, compared to changes evident from microarray data published in the literature (50).

Finally, the initial set-up included four additional genes, which all have been shown to be affected by various types of delivery systems in macrophages, namely the cytokines IL-6, IL-17 F and IFN-γ as well as oligoadenylate synthetase-like protein 1 d (OAS1d), which is induced upon interferon activation by double-stranded RNA (36,51–53). However, the expression levels were too low for accurate primer validation with Trans-IT-TKO under the current experimental conditions (data not shown).

DISCUSSION

A number of different polymeric carriers has been used for siRNA delivery, but it is generally difficult to compare silencing and non-specific effects obtained in different studies due to highly variable experimental conditions such as the cell type and transfection protocol, including incubation time and the presence of serum proteins that tend to destabilize cationic nanocarriers, and polyplexes in particular (54,55). Therefore, comparative and carefully performed studies like the current investigation are highly needed.

A remarkably high level of TNF-α silencing for the PAMAM G7 dendrimer (96%) and the nanogels (90%) was observed, which was superior to previous investigations of the same systems (70–80% and 45% for the nanogels and PAMAM G7, respectively) (19,20). On the other hand, a former study of the comparable triethanolamine core PAMAM dendrimers showed 80% silencing with G7, whereas there was little effect of the dendrimers corresponding to G4 (20). Presently, the PEGylated nanogels and PAMAM G4 dendrimers also mediated high gene silencing (75–85%), which was equal or superior to previous findings (19,20,44). Less efficient silencing (below 40%) was observed for pHPMA-MPPM polyplexes and DOTAP-modified PLGA nanoparticles, compared to previous findings (39,45), while a similar level of silencing (40%) was observed for TMC-SH. In the latter case, improved silencing has been observed by incubation under serum-free conditions (Table I) (42). However, it should be noted that silencing in this study was given as the difference in the TNF-α expression between cells treated with carriers containing the specific TNF-α and the non-specific control siRNA sequences, that in some cases have been shown to up-regulate target gene expression, while previous studies with polyplexes have normalized gene silencing directly to untreated controls (19,39,42). This may explain the differences in observed silencing. The difference can also depend on polymer and nanogel batch-to-batch variations or more importantly, differences in cell lines and transfection protocols. For example a macrophage cell line was used in the current study, enabling phagocytotic uptake of the nanocarriers, and LPS was added to activate the cells (56). In addition, the present protocol of 24 h incubation with siRNA nanocarriers is shorter than the 2–3 days transfection period used in previous studies (Table I). This further demonstrates the importance of testing different systems in the same model to enable a direct evaluation of differences in transfection efficiency between systems.

Four different types of polyplexes and three different nanosphere-based delivery systems were tested in the current study. In general, there was no overall difference in the transfection capabilities between polyplexes and nanospheres. However, it was evident that some structural features affected the level of silencing (Table I, Fig. 2). In detail, a high charge density facilitated increased silencing for the PAMAM dendrimers, corresponding to previous findings (19). An effect of PEGylation was observed for the nanogels, which reduced the silencing efficiency, potentially due to the reduced surface charge, resulting in lower cellular uptake (44,57). In line with this, there was a general tendency towards decreased transfection efficiency of the more stable or stabilized nanocarrier systems. These include the TMC-SH and pHPMA-MPPM polymer carriers, for which the colloidal stability has been improved via chemical modifications, and the DOTAP-modified PLGA polymeric matrix nanoparticles (28,40,41). This represents a dilemma in the field that particle stabilization and charge shielding often results in reduced target cell uptake, drug release, and membrane destabilization when tested *in vitro* (58), but the decreased transfection efficiency may also be a result of shorter incubation time with the nanocarriers, compared to previous reports (Table I).

For the polyplexes, a rather fast release of siRNA is expected. However, for the DOTAP-modified PLGA nanoparticles and the nanogels, a sustained release of siRNA has been observed (unpublished results). For unmodified PLGA nanoparticles we have recently demonstrated a burst release of surface-localized siRNA followed by a triphasic sustained release (28). However, our unpublished studies suggest that the siRNA release profile is changed by modification with DOTAP towards a lower burst release due to a reduced amount of siRNA present on the nanoparticle surface followed by a faster release of the siRNA from the nanoparticles once taken up into the cells. For the dextran gels, the release of siRNA was initially investigated in the context of controlled siRNA release from dextran microgels (59). These experiments indicated that the release of the siRNA from the gels was degradation-controlled. Although no data is available on the siRNA release from dextran nanogels, dextran nanogels were shown to degrade as a function of time (27,44). This degradation was shown to depend on the crosslink density of the gels (and therefore the degree of substitution of the dex-MA or dex-HEMA). It has also been shown that the crosslink density influences siRNA loading and gene silencing efficacy (60). Although dex-MA gels do not degrade as a function of time, reasonably good transfection efficiency is observed. The authors believe that this could be caused by the interaction between the nanogels and (negatively charged) intracellular compounds. These compounds may displace nanogel loaded siRNA molecules (especially in the outer shell), which can then initiate gene silencing.

Another important issue to address when working with siRNA delivery, is the level of toxicity, which was measured

by annexin V and PI staining. We found a concentration-dependent reduction in the number of viable cells upon exposure to siRNA-formulated nanocarriers with less than 15% reduction for the majority of the polymers (Fig. 3a), compared to 10% in previous reports (19,27,42,44,45). Polyplexes formulated with pHPMA-MPPM induced a drastic decrease in viability at 50–100 nM siRNA, reaching 46% toxicity, which was in contrast to the previously reported 18% toxicity at 80 nM siRNA at a similar N/P ratio (39). As expected, the polymeric nanocarriers displayed a concentration-dependent toxicity, except for PAMAM G4, which showed no decrease in viability in the examined concentration range. Within the population of viable cells, cells undergoing early apoptosis are included, displaying early signs of toxicity. siRNA delivery with TMC-SH and DOTAP-modified PLGA nanoparticles induced more than 5% of early apoptotic cells, which indicates that even though toxicity is low, cellular changes have occurred (Fig. 3b). We have recently shown that the toxicity induced by the DOTAP-modified PLGA nanocarriers is caused by the DOTAP component in a concentration-dependent way (45). The minor increase in observed toxicity in the current experiments may also be a result of the reverse transfection protocol, since cell harvesting by scraping can cause membrane damage. Such membrane damage may also make the cells more susceptible to transfection by increasing the membrane permeability, which could also explain the silencing induced by the naked siRNA (30%, Fig. 2).

In recent years, an increasing number of studies have focused on the adverse effects of nanomedicine and gene delivery (33), which are observed both *in vitro* and *in vivo* (61). Multiple studies have evaluated the changes in gene expression patterns by microarray analysis (32,35,36,50,62–64). We used a different approach for investigating selected off-target effects of polymeric siRNA nanocarriers, and included a panel of five genes, which have previously shown changed gene expression upon nanocarrier exposure (Table II). The strength of the current setup, compared to previous microarray studies, is that the nanocarrier dose-dependency is also accounted for in the analysis. However, we demonstrate only minor changes in gene regulation under the applied experimental conditions (Table V).

Some of the changes in gene regulation indicated a concentration-dependent effect, as decreased (Il-1β, Cd14) and increased (Cse1L) expression was observed with increased carrier concentration for the majority of nanocarrier systems resulting in expression levels comparable to the expression levels in non-activated cells. This may indicate that the siRNA nanocarriers counteract the LPS-induced activation, which could be a downstream effect of the siRNA-mediated silencing of the proinflammatory cytokine. However, when evaluating the present deregulation mediated by the PAPMAM dendrimers and nanogels, which induced high TNF-α silencing, the changes in gene regulation were not uni-directed, indicating that the changes are mediated by the polymers in formulation with siRNA.

The protein products for the selected genes are involved in different regulatory pathways, including the inflammatory response (IL-1β), innate immune response (CD14), apoptosis/proliferation (CSE1L) and proliferation (CDK7 and CCNA2) (Table II). The only gene that displayed pronounced down-regulation by multiple carriers was Il-1β, which indicates a reduced inflammatory response upon nanocarrier-mediated siRNA delivery (Table V).

We evaluated siRNA delivery to the murine macrophage cell line RAW 264.7 *in vitro* using siRNA directed against the clinically relevant RA target TNF-α and demonstrated high levels of gene silencing and low toxicity of PAMAM dendriplexes and dextran nanogel-mediated siRNA delivery. TNF-α silencing has previously been demonstrated in this cell line upon siRNA delivery using chitosan nanoparticles (37), which furthermore improved joint characteristics in collagen-induced arthritic mice after intraperitoneal administration (10,37). This provides for an *in vivo* proof-of-concept for polymeric siRNA nanocarriers, and it would therefore be interesting to test the currently tested nanocarriers *in vivo*, to evaluate if the present *in vitro* ranking of carriers mediating high and low siRNA silencing is comparable to silencing in a preclinical model of RA.

CONCLUSION

The current study comprises a direct comparison of seven polymer-based nanocarriers for transfecting the LPS-activated macrophage cell line RAW 264.7 with a therapeutically relevant siRNA. We demonstrate a highly specific *in vitro* gene silencing and low toxicity of PAMAM dendriplexes and non-PEGylated and PEGylated nanogels loaded with siRNA, whereas TMC-SH, pHPMA-MPPM and DOTAP-modified PLGA nanoparticles were less effective as carriers for siRNA transfection. Expression analysis of five off-target genes was performed to examine adverse effects of the siRNA transfection, and only minor transcriptional changes were observed. This suggests that the siRNA carrier systems investigated are well tolerated *in vitro*, and that PAMAM dendrimers and dextran nanogels formulated with siRNA are very potent carriers for silencing TNF-α gene expression *in vitro*.

ACKNOWLEDGMENTS & DISCLOSURES

We gratefully thank Kirsten Vikkelsø Madsen for valuable scientific discussions concerning real time RT-PCR, Lasse Bengtson for preparation of the DOTAP/PLGA nano-

particles, and Dr. Michael Timm for testing pyrogen levels of the delivery systems (all from the Faculty of Pharmaceutical Sciences, University of Copenhagen). This study has been carried out with financial support from the Commission of the European Communities, Priority 3 "Nanotechnologies and Nanosciences, Knowledge Based Multifunctional Materials, New Production Processes and Devices" of the Sixth Framework Programme for Research and Technological Development (Targeted Delivery of Nanomedicine: NMP4-CT-2006-026668). We are grateful to the Danish Agency for Science, Technology and Innovation, the Drug Research Academy and the Carlsberg Foundation for financial support for the Zetasizer Nano ZS, Nanodrop 2000 C Spectrophotometer and the LightCycler® 480 system, respectively. The funding sources had no involvement in the study design, in the collection, analysis and interpretation of data, just as they had no involvement in the writing of the report and the decision to submit the paper for publication.

REFERENCES

1. Doan T, Massarotti E. Rheumatoid arthritis: An overview of new and emerging therapies. J Clin Pharmacol. 2005;45(7):751–62.
2. Kinne RW, Brauer R, Stuhlmuller B, Palombo-Kinne E, Burmester GR. Macrophages in rheumatoid arthritis. Arthritis Res. 2000;2(3):189–202.
3. Kinne RW, Stuhlmuller B, Burmester GR. Cells of the synovium in rheumatoid arthritis—Macrophages. Arthritis Res Ther. 2007;9(6).
4. Scott DL, Kingsley GH. Tumor necrosis factor inhibitors for rheumatoid arthritis. N Engl J Med. 2006;355(7):704–12.
5. van Vollenhoven RF. Treatment of rheumatoid arthritis: state of the art 2009. Nat Rev Rheumatol. 2009;5(10):531–41.
6. Huber LC, Distler O, Gay RE, Gay S. Antisense strategies in degenerative joint diseases: Sense or nonsense? Adv Drug Deliv Rev. 2006;58(2):285–99.
7. Khoury M, Jorgensen C, Apparailly F. RNAi in arthritis: Prospects of a future antisense therapy in inflammation. Curr Opin Mol Ther. 2007;9(5):483–9.
8. Castanotto D, Rossi JJ. The promises and pitfalls of RNA-interference-based therapeutics. Nature. 2009;457(7228):426–33.
9. Schiffelers RM, Xu J, Storm G, Woodle MC, Scaria PV. Effects of treatment with small interfering RNA on joint inflammation in mice with collagen-induced arthritis. Arthritis Rheum. 2005;52(4):1314–8.
10. Howard KA, Paludan SR, Behlke MA, Besenbacher F, Deleuran B, Kjems J. Chitosan/siRNA nanoparticle-mediated TNF-alpha knockdown in peritoneal macrophages for anti-inflammatory treatment in a murine arthritis model. Mol Ther. 2009;17(1):162–8.
11. Khoury M, Louis-Plence P, Escriou V, Noel D, Largeau C, Cantos C, *et al.* Efficient new cationic liposome formulation for systemic delivery of small interfering RNA silencing tumor necrosis factor alpha in experimental arthritis. Arthritis Rheum. 2006;54(6):1867–77.
12. Khoury M, Courties G, Fabre S, Bouffi C, Seemayer CA, Vervoordeldonk MJ, *et al.* Adeno-associated virus type 5-mediated intraarticular administration of tumor necrosis factor small interfering RNA improves collagen-induced arthritis. Arthritis Rheum. 2010;62(3):765–70.
13. Scaggiante B, Dapas B, Farra R, Grassi M, Pozzato G, Giansante C, *et al.* Improving siRNA bio-distribution and minimizing side effects. Curr Drug Metab. 2011;12(1):11–23.
14. Whitehead KA, Langer R, Anderson DG. Knocking down barriers: advances in siRNA delivery. Nat Rev Drug Discov. 2009;8(2):129–38.
15. Cun D, Jensen LB, Nielsen HM, Moghimi M, Foged C. Polymeric nanocarriers for siRNA delivery: Challenges and future prospects. J Biomed Nanotechnol. 2008;4(3):258–75.
16. Mislick KA, Baldeschwieler JD. Evidence for the role of proteoglycans in cation-mediated gene transfer. Proc Natl Acad Sci USA. 1996;93(22):12349–54.
17. Urban-Klein B, Werth S, Abuharbeid S, Czubayko F, Aigner A. RNAi-mediated gene-targeting through systemic application of polyethylenimine (PEI)-complexed siRNA *in vivo*. Gene Ther. 2005;12(5):461–6.
18. Werth S, Urban-Klein B, Dai L, Hobel S, Grzelinski M, Bakowsky U, *et al.* A low molecular weight fraction of polyethylenimine (PEI) displays increased transfection efficiency of DNA and siRNA in fresh or lyophilized complexes. J Control Release. 2006;112(2):257–70.
19. Perez AP, Romero EL, Morilla MJ. Ethylendiamine core PAMAM dendrimers/siRNA complexes as *in vitro* silencing agents. Int J Pharm. 2009;380(1–2):189–200.
20. Zhou JH, Wu JY, Hafdi N, Behr JP, Erbacher P, Peng L. PAMAM dendrimers for efficient siRNA delivery and potent gene silencing. Chem Comm. 2006;22:2362–4.
21. Duncan R, Izzo L. Dendrimer biocompatibility and toxicity. Adv Drug Deliv Rev. 2005;57(15):2215–37.
22. Lv H, Zhang S, Wang B, Cui S, Yan J. Toxicity of cationic lipids and cationic polymers in gene delivery. J Control Release. 2006;114(1):100–9.
23. Luten J, van Nostruin CF, De Smedt SC, Hennink WE. Biodegradable polymers as non-viral carriers for plasmid DNA delivery. J Control Release. 2008;126(2):97–110.
24. Kim TH, Jiang HL, Jere D, Park IK, Cho MH, Nah JW, *et al.* Chemical modification of chitosan as a gene carrier *in vitro* and *in vivo*. Progr Polymer Sci. 2007;32(7):726–53.
25. Lee KY. Chitosan and its derivatives for gene delivery. Macromol Res. 2007;15(3):195–201.
26. Raemdonck K, Demeester J, De Smedt S. Advanced nanogel engineering for drug delivery. Soft Matter. 2009;5(4):707–15.
27. Raemdonck K, Naeye B, Buyens K, Vandenbroucke RE, Hogset A, Demeester J, *et al.* Biodegradable dextran nanogels for RNA interference: Focusing on endosomal escape and intracellular siRNA delivery. Adv Funct Mater. 2009;19(9):1406–15.
28. Cun D, Jensen DK, Maltesen MJ, Bunker M, Whiteside P, Scurr D, *et al.* High loading efficiency and sustained release of siRNA encapsulated in PLGA nanoparticles: quality by design optimization and characterization. Eur J Pharm Biopharm. 2011;77(1):26–35.
29. Jackson AL, Linsley PS. Recognizing and avoiding siRNA off-target effects for target identification and therapeutic application. Nat Rev Drug Discov. 2010;9(1):57–67.
30. Robbins M, Judge A, MacLachlan I. siRNA and innate immunity. Oligonucleotides. 2009;19(2):89–102.
31. Judge A, MacLachlan I. Overcoming the innate immune response to small interfering RNA. Hum Gene Ther. 2008;19(2):111–24.
32. Omidi Y, Hollins AJ, Benboubetra M, Drayton R, Benter IF, Akhtar S. Toxicogenomics of non-viral vectors for gene therapy: A microarray study of lipofectin- and oligofectamine-induced gene expression changes in human epithelial cells. J Drug Target. 2003;11(6):311–23.

33. Akhtar S. Cationic nanosystems for the delivery of small interfering ribonucleic acid therapeutics: a focus on toxicogenomics. Expert Opin Drug Metab Toxicol. 2010;6(11):1347–62.
34. Akhtar S, Benter I. Toxicogenomics of non-viral drug delivery systems for RNAi: Potential impact on siRNA-mediated gene silencing activity and specificity. Adv Drug Deliv Rev. 2007;59(2–3):164–82.
35. Hollins AJ, Omidi Y, Benter IF, Akhtar S. Toxicogenomics of drug delivery systems: Exploiting delivery system-induced changes in target gene expression to enhance siRNA activity. J Drug Target. 2007;15(1):83–8.
36. Gras R, Almonacid L, Ortega P, Serramia MJ, Gomez R, de la Mata FJ, *et al.* Changes in gene expression pattern of human primary macrophages induced by carbosilane dendrimer 2G-NN16. Pharm Res. 2009;26(3):577–86.
37. Andersen MO, Howard KA, Paludan SR, Besenbacher F, Kjems J. Delivery of siRNA from lyophilized polymeric surfaces. Biomaterials. 2008;29(4):506–12.
38. Amarzguioui M, Lundberg P, Cantin E, Hagstrom J, Behlke MA, Rossi JJ. Rational design and *in vitro* and *in vivo* delivery of Dicer substrate siRNA. Nat Protoc. 2006;1(2):508–17.
39. Varkouhi AK, Lammers T, Schiffelers RM, van Steenbergen MJ, Hennink WE, Storm G. Gene silencing activity of siRNA polyplexes based on biodegradable polymers. Eur J Pharm Biopharm. 2011;77(3):450–7.
40. Verheul RJ, van der Wal S, Hennink WE. Tailorable thiolated trimethyl chitosans for covalently stabilized nanoparticles. Biomacromolecules. 2010;11(8):1965–71.
41. Luten J, Akeroyd N, Funhoff A, Lok MC, Talsma H, Hennink WE. Methacrylamide polymers with hydrolysis-sensitive cationic side groups as degradable gene carriers. Bioconjug Chem. 2006;17(4):1077–84.
42. Varkouhi AK, Verheul RJ, Schiffelers RM, Lammers T, Storm G, Hennink WE. Gene silencing activity of siRNA polyplexes based on thiolated N, N, N-trimethylated chitosan. Bioconjug Chem. 2010;21(12):2339–46.
43. Jensen LB, Mortensen K, Pavan GM, Kasimova MR, Jensen DK, Gadzhyeva V, *et al.* Molecular characterization of the interaction between siRNA and PAMAM G7 dendrimers by SAXS, ITC, and molecular dynamics simulations. Biomacromolecules. 2010;11(12):3571–7.
44. Naeye B, Raemdonck K, Remaut K, Sproat B, Demeester J, De Smedt SC. PEGylation of biodegradable dextran nanogels for siRNA delivery. Eur J Pharm Sci. 2010;40(4):342–51.
45. Jensen DK, Jensen LB, Koocheki S, *et al.* Design of an inhalable dry powder formulation of DOTAP-modified PLGA nanoparticles loaded with siRNA. J Control Release. 2011;In press.
46. Timm M, Hansen EW, Moesby L, Christensen JD. Utilization of the human cell line HL-60 for chemiluminescence based detection of microorganisms and related substances. Eur J Pharm Sci. 2006;27(2–3):252–8.
47. Pfaffl MW. A new mathematical model for relative quantification in real-time RT-PCR. Nucl Acids Res. 2001;29(9).
48. Chapekar MS, Zaremba TG, Kuester RK, Hitchins VM. Synergistic induction of tumor necrosis factor alpha by bacterial lipopolysaccharide and lipoteichoic acid in combination with polytetrafluoroethylene particles in a murine macrophage cell line RAW 264.7. J Biomed Mater Res. 1996;31(2):251–6.
49. Amarzguioui M. Improved siRNA-mediated silencing in refractory adherent cell lines by detachment and transfection in suspension. Biotechniques. 2004;36(5):766–8.
50. Barar J, Hamzeiy H, Tabatabaei SAM, Hashemi-Aghdam SE, Omidi Y. Genomic signature and toxicogenomics comparison of polycationic gene delivery nanosystems in human alveolar epithelial A549 cells. Daru. 2009;17(3):139–47.
51. Saito Y, Higuchi Y, Kawakami S, Yamashita F, Hashida M. Immunostimulatory characteristics induced by linear polyethyleneimine-plasmid DNA complexes in cultured macrophages. Hum Gene Ther. 2009;20(2):137–45.
52. Shell SA, Hesse C, Morris SM, Milcarek C. Elevated levels of the 64-kDa cleavage stimulatory factor (CstF-64) in lipopolysaccharide-stimulated macrophages influence gene expression and induce alternative poly(A) site selection. J Biol Chem. 2005;280(48):39950–61.
53. Yan W, Ma L, Stein P, Pangas SA, Burns KH, Bai Y, *et al.* Mice deficient in oocyte-specific oligoadenylate synthetase-like protein OAS1D display reduced fertility. Mol Cell Biol. 2005;25(11):4615–24.
54. Merkel OM, Librizzi D, Pfestroff A, Schurrat T, Buyens K, Sanders NN, *et al.* Stability of siRNA polyplexes from poly(ethylenimine) and poly(ethylenimine)-g-poly(ethylene glycol) under *in vivo* conditions: effects on pharmacokinetics and biodistribution measured by Fluorescence Fluctuation Spectroscopy and Single Photon Emission Computed Tomography (SPECT) imaging. J Control Release. 2009;138(2):148–59.
55. Buyens K, Meyer M, Wagner E, Demeester J, De Smedt SC, Sanders NN. Monitoring the disassembly of siRNA polyplexes in serum is crucial for predicting their biological efficacy. J Control Release. 2010;141(1):38–41.
56. Brunner T, Cohen S, Monsonego A. Silencing of proinflammatory genes targeted to peritoneal-residing macrophages using siRNA encapsulated in biodegradable microspheres. Biomaterials. 2010;31(9):2627–36.
57. Owens DE, Peppas NA. Opsonization, biodistribution, and pharmacokinetics of polymeric nanoparticles. Int J Pharm. 2006;307(1):93–102.
58. Millili PG, Selekman JA, Blocker KM, Johnson DA, Naik UP, Sullivan MO. Structural and functional consequences of poly(ethylene glycol) inclusion on DNA condensation for gene delivery. Microsc Res Tech. 2010;73(9):866–77.
59. Raemdonck K, Van Thienen TG, Vandenbroucke RE, Sanders NN, Demeester J, De Smedt SC. Dextran microgels for time-controlled delivery of siRNA. Adv Funct Mater. 2008;18(7):993–1001.
60. Raemdonck K, Naeye B, Hogset A, Demeester J, De Smedt SC. Prolonged gene silencing by combining siRNA nanogels and photochemical internalization. J Control Release. 2010;145(3):281–8.
61. Armstrong ME, Gantier M, Li LL, Chung WY, McCann A, Baugh JA, *et al.* Small interfering RNAs induce macrophage migration inhibitory factor production and proliferation in breast cancer cells via a double-stranded RNA-dependent protein kinase-dependent mechanism. J Immunol. 2008;180(11):7125–33.
62. Omidi Y, Barar J, Heidari HR, Ahmadian S, Yazdi HA, Akhtar S. Microarray analysis of the toxicogenomics and the genotoxic potential of a cationic lipid-based gene delivery nanosystem in human alveolar epithelial A549 cells. Toxicol Mech Method. 2008;18(4):369–78.
63. Omidi Y, Hollins AJ, Drayton RM, Akhtar S. Polypropylenimine dendrimer-induced gene expression changes: The effect of complexation with DNA, dendrimer generation and cell type. J Drug Target. 2005;13(7):431–43.
64. Kuo JHS, Liou MJ, Chiu HC. Evaluating the gene-expression profiles of HeLa cancer cells treated with activated and nonactivated poly(amidoamine) dendrimers, and their DNA complexes. Mol Pharm. 2010;7(3):805–14.
65. Vannucci L, Fiserova A, Sadalapure K, Lindhorst TK, Kuldova M, Rossmann P, *et al.* Effects of N-acetyl-glucosamine-coated glycodendrimers as biological modulators in the B16F10 melanoma model *in vivo*. Int J Oncol. 2003;23(2):285–96.
66. Tai CJ, Hsu CH, Shen SC, Lee WR, Jiang MC. Cellular apoptosis susceptibility (CSE1L/CAS) protein in cancer metastasis and chemotherapeutic drug-induced apoptosis. J Exp Clin Cancer Res. 2010;29.